



Universiteit
Leiden
The Netherlands

Prognostic implications of right ventricular systolic dysfunction in cardiac amyloidosis

Tjahjadi, C.; Fortuni, F.; Stassen, J.; Debonnaire, P.; Lustosa, R.P.; Marsan, N.A.; ... ; Bax, J.J.

Citation

Tjahjadi, C., Fortuni, F., Stassen, J., Debonnaire, P., Lustosa, R. P., Marsan, N. A., ... Bax, J. J. (2022). Prognostic implications of right ventricular systolic dysfunction in cardiac amyloidosis. *American Journal Of Cardiology*, 173, 120-127. doi:10.1016/j.amjcard.2022.02.048

Version: Publisher's Version
License: [Creative Commons CC BY 4.0 license](https://creativecommons.org/licenses/by/4.0/)
Downloaded from: <https://hdl.handle.net/1887/3567729>

Note: To cite this publication please use the final published version (if applicable).

Prognostic Implications of Right Ventricular Systolic Dysfunction in Cardiac Amyloidosis



Catherina Tjahjadi, MD^a, Federico Fortuni, MD^{a,b}, Jan Stassen, MD^{a,c},
Philippe Debonnaire, MD, PhD^{a,d}, Rodolfo P. Lustosa, MD^a, Nina Ajmone Marsan, MD, PhD^a,
Victoria Delgado, MD, PhD^a, and Jeroen J. Bax, MD, PhD^{a,*}

Left ventricular (LV) systolic dysfunction in cardiac amyloidosis (CA) is associated with poor prognosis. This study aimed to investigate the prognostic implications of right ventricular (RV) systolic dysfunction in CA. A total of 93 patients diagnosed with CA who underwent standard and speckle-tracking echocardiography were included. During a median follow-up of 17 (5 to 38) months, 42 patients (45%) died. Nonsurvivors were more likely to present with immunoglobulin light-chain amyloidosis and New York Heart Association class III to IV heart failure symptoms. Regarding the echocardiographic characteristics, nonsurvivors had a higher LV apical ratio, worse LV diastolic function, and worse RV systolic function (evaluated with both tricuspid annular plane systolic excursion and RV free wall strain). RV free wall strain was independently associated with all-cause mortality in several multivariable Cox regression models and had incremental prognostic value over conventional parameters of RV function when added to a basal model (including heart failure symptoms, amyloidosis phenotype, and LV global longitudinal strain). Based on spline curve analysis and Youden index, a value of 16% for RV free wall strain was identified as the optimal cutoff to predict outcome and patients with RV free wall strain <16% had a significantly worse short- and long-term survival during follow-up (1- and 3-year cumulative survival: 81% vs 31% and 67% vs 20%, respectively, $p < 0.001$). In conclusion, RV systolic dysfunction is independently associated with poor outcome in patients with CA and the use of advanced echocardiographic parameters, such as RV free wall strain, may be of aid for better risk stratification. © 2022 The Author(s). Published by Elsevier Inc. This is an open access article under the CC BY license (<http://creativecommons.org/licenses/by/4.0/>) (Am J Cardiol 2022;173:120–127)

Introduction

Amyloidosis is a clinical condition caused by the deposition of extracellular misfolded protein aggregates that interfere with the normal structure and function of the involved organs.¹ There are different types of amyloidosis depending on the precursor protein with 2 main forms affecting the heart: immunoglobulin light-chain amyloidosis (AL) and transthyretin (ATTR) amyloidosis.^{2,3}

^aDepartment of Cardiology, Leiden University Medical Center, Leiden, The Netherlands; ^bDepartment of Cardiology, San Giovanni Battista Hospital, Foligno, Italy; ^cDepartment of Cardiology, Jessa Hospital, Hasselt, Belgium; and ^dDepartment of Cardiology, Sint-Jan Hospital Bruges, Bruges, Belgium. Manuscript received December 30, 2021; revised manuscript received and accepted February 22, 2022.

Drs. Tjahjadi and Fortuni contributed equally as co-first authors.

Dr. Stassen received funding from the European Society of Cardiology (Brussels, Belgium), training grant App000064741. The Department of Cardiology of the Leiden University Medical Center received research grants from Abbott Vascular (Chicago, Illinois), Bayer (Leverkusen, Germany), BioVentric (San Ramon, California), Medtronic (Dublin, Ireland), Biotronik (Berlin, Germany), Boston Scientific (Marlborough, Massachusetts), GE Healthcare (Chicago, Illinois), and Edwards Lifesciences (Irvine, California).

See page 126 for disclosure information.

*Corresponding author: Tel: +31 71 526 2020; fax: +31 71 526 6809.

E-mail address: j.j.bax@lumc.nl (J.J. Bax).

Cardiac infiltration is the major determinant of survival regardless of the subtype of amyloidosis.⁴ Early diagnosis is important to timely implement therapy and to improve outcomes but challenging because the symptoms are non-specific in the early stages. A high degree of suspicion, particularly when there is multiorgan involvement and/or unexplained heart failure with preserved ejection fraction (EF) determines further evaluation and management. With the increasing use of advanced noninvasive cardiac imaging techniques, diagnosis could be enhanced and prognostic markers better identified. Echocardiography is an easily accessible tool and often the first-line imaging modality used to investigate patients with unexplained heart failure symptoms. Cardiac amyloidosis (CA) is a biventricular disease. The prognostic implications of left ventricular (LV) systolic dysfunction in CA are well established. However, there are only few studies looking into the association between right ventricular (RV) systolic function and survival.^{5,6} In addition, other pathologies that may resemble CA, such as hypertensive cardiomyopathy and hypertrophic cardiomyopathy, can also affect the LV. In these situations, assessment of the RV could help in the differential diagnosis.³ In this study, the association between standard and advanced echocardiographic parameters of LV and RV systolic function and all-cause mortality were investigated.

Methods

Patients diagnosed with CA who underwent echocardiographic assessment at the Leiden University Medical Center (The Netherlands) or at AZ Sint-Jan Hospital Bruges (Belgium) between April 1999 and December 2019 were retrospectively included in the present study. The diagnosis of CA was based on either endomyocardial biopsy or extracardiac biopsy with typical cardiac imaging features.⁷ The study complies with the Declaration of Helsinki and received the approval of the institutional review boards. The medical ethical committee of both hospitals waived the need of written informed consent because of the retrospective nature of this study.

Transthoracic echocardiographic images were recorded using Vivid 7 or E9 ultrasound system (General Electric Vingmed Ultrasound, Milwaukee, Wisconsin) with patients at rest in the left lateral decubitus. Echocardiographic data were stored and measured offline using dedicated software (EchoPac version 204, General Electric Vingmed Ultrasound). Parasternal, apical, and subcostal views were used to acquire 2-dimensional, color, pulsed, and continuous wave Doppler data according to current recommendations.⁸ Standard conventional echocardiographic and 2-dimensional speckle-tracking echocardiography-derived strain measurements were performed in accordance with the most recent American Society of Echocardiography and the European Association of Cardiovascular Imaging guidelines.⁸ LV end-systolic and end-diastolic volumes were measured on the apical 2- and 4-chamber views and LVEF was calculated according to Simpson biplane method.⁸ The apical 2-, 3-, and 4-chamber views were used to derive LV global longitudinal strain (GLS). LV apical ratio was calculated as the ratio between the average apical strain values and the average of basal and midventricular strain values. Mitral and tricuspid valve regurgitation were assessed according to current guidelines and graded as mild, moderate, or severe.⁹ RV dimensions (including basal, midcavity, and longitudinal diameters) were measured at end-diastole according to the current guidelines. Anatomical M-mode was applied on the focused apical 4-chamber view of the RV to measure tricuspid annular plane systolic excursion (TAPSE). RV strain analysis was obtained from the RV-focused apical 4-chamber view with the reference point placed at the beginning of the QRS complex. The endocardial border was traced automatically by the software after setting the reference points at the septal and lateral borders of the tricuspid annulus and the apex. The automatic tracings were adjusted manually to ensure optimal tracking throughout the cardiac cycle. The RV free wall strain was calculated as the average value from the 3 RV free wall segments.¹⁰ Pulmonary artery systolic pressure was derived from the peak tricuspid regurgitation velocity using the simplified Bernoulli equation, adding the right atrial pressure estimated from inferior vena cava diameter and collapsibility.⁸ In patients with atrial fibrillation, for all echocardiographic measurements, the average of 3 to 5 beats was considered.

Low-voltage ECG was defined as a QRS voltage amplitude ≤ 0.5 mV in all limb leads, ≤ 1 mV in all precordial leads, or the sum of the S wave in V_1 and R wave in V_5 or $V_6 < 1.5$ mV.¹¹

All patients were followed up for the occurrence of all-cause mortality. Survival data were ascertained from the Social Security Death Index and medical records and were complete for all patients.

Statistical analysis was performed using SPSS version 25.0 (SPSS, Armonk, New York) and in R environment (version 4.0.1, R Foundation for Statistical Computing). Normality was visually assessed by comparing histograms of the sample data to a normal probability curve. Continuous variables were presented as mean \pm SD or median and interquartile range as appropriate. Categorical variables were reported as frequencies and percentages. The differences between survivors and nonsurvivors during the follow-up were compared using the *t* test and Mann-Whitney *U* test for continuous variables and the chi-square test for categorical variables. Considering the limited number of events and to avoid overfitting of the models, several multivariable Cox proportional hazard regression analyses were performed to assess the clinical and echocardiographic factors that were independently associated with all-cause mortality. Possible confounders with a significant *p* value (< 0.05) in the univariable analysis were included in the multivariable regression analysis. Hazard ratios (HRs) and 95% confidence intervals were calculated. A spline curve was fitted to assess the HR change for all-cause mortality across a range of RV free wall strain values. Receiver operating characteristic curve was used to characterize the prognostic value of RV free wall strain to predict survival. The Youden index and the spline curve analysis were used to define a prognostic relevant cut-off value of RV free wall strain. The Kaplan-Meier curves were used to estimate the 1- and 3-year survival rates, and differences between groups were analyzed using the log-rank test. A 2-sided *p* < 0.05 was considered statistically significant.

Results

A total of 93 patients with CA were included in the present study. Endomyocardial biopsy-proved diagnosis was available in 39 patients (42%) and the remaining patients were diagnosed by extracardiac biopsy with characteristic cardiac features on echocardiography, cardiac magnetic resonance, or bone scintigraphy imaging. During a median follow-up of 17 (5 to 38) months, 42 patients (45%) died. The baseline clinical characteristics of the overall population, survivors, and nonsurvivors are presented in [Table 1](#). Overall, the median age was 73 (63 to 80) years, 73% were male, 27% presented with New York Heart Association (NYHA) class III to IV heart failure symptoms and more than half of the patients (55%) had chronic kidney disease. In the per-group analysis, survivors had similar age, cardiovascular risk factors, and co-morbidities compared with nonsurvivors. However, compared with survivors, patients who died during follow-up were more likely to be diagnosed with AL amyloidosis had more severe heart failure symptoms (i.e., NYHA class III to IV) and used less angiotensin-converting enzyme inhibitors or angiotensin-II receptor blockers.

The conventional and deformation echocardiographic parameters are presented in [Table 2](#). Overall, the mean LV mass and RV free wall thickness were increased, mean left

Table 1
Clinical characteristics

| Variable | Total (n=93) | Survivors (n=51) | Nonsurvivors (n=42) | p value |
|--|--------------|------------------|---------------------|---------|
| Age, years | 73 (63–80) | 77 (66–81) | 69 (61–78) | 0.064 |
| Men | 68 (73%) | 38 (75%) | 30 (71%) | 0.739 |
| Amyloid light-chain phenotype | 31 (33%) | 10 (20%) | 21 (50%) | 0.002 |
| Amyloid transthyretin phenotype | 47 (51%) | 35 (69%) | 12 (29%) | <0.001 |
| Low QRS voltage | 33 (36%) | 13 (26%) | 20 (49%) | 0.021 |
| New York Heart Association class III-IV | 25 (27%) | 8 (16%) | 17 (41%) | 0.007 |
| Body mass index (kg/m ²) | 25 ± 4 | 25 ± 4 | 24 ± 4 | 0.103 |
| Diabetes mellitus | 16 (17%) | 10 (20%) | 6 (14%) | 0.499 |
| Hypertension | 46 (50%) | 31 (61%) | 15 (36%) | 0.016 |
| Dyslipidemia | 34 (37%) | 23 (45%) | 11 (26%) | 0.060 |
| Current or former smoker | 28 (30%) | 17 (33%) | 11 (26%) | 0.455 |
| Atrial fibrillation | 23 (25%) | 12 (24%) | 11 (26%) | 0.767 |
| Family history of coronary artery disease | 10 (11%) | 6 (12%) | 4 (10%) | 0.728 |
| Coronary artery disease | 21 (23%) | 14 (28%) | 7 (17%) | 0.238 |
| Chronic kidney disease | 51 (55%) | 29 (57%) | 22 (52%) | 0.666 |
| Polyneuropathy | 8 (9%) | 4 (8%) | 4 (10%) | 0.774 |
| Beta blocker | 44 (47%) | 27 (53%) | 17 (41%) | 0.231 |
| Anti-arrhythmic | 9 (10%) | 4 (8%) | 5 (12%) | 0.510 |
| Renin angiotensin aldosterone system inhibitor | 38 (41%) | 26 (51%) | 12 (29%) | 0.029 |
| Diuretic | 61 (66%) | 30 (59%) | 31 (74%) | 0.130 |
| Mineralocorticoid receptor antagonists | 29 (31%) | 16 (31%) | 13 (31%) | 0.965 |
| Statin | 40 (43) | 28 (55) | 12 (29) | 0.011 |

atrial volumes were dilated, LV filling pressures were increased (mean $E/e' > 14$) in 51% of the patients and mean pulmonary pressures were slightly above the upper normal range. The median LVEF was preserved, whereas more advanced parameters of LV systolic function, such as mean LV GLS, were impaired. In the per-group analysis, nonsurvivors had smaller left and right atrial volumes, lower stroke volume, higher LV apical ratio, and more impaired

indexes of LV diastolic function than survivors. In addition, patients who died during follow-up had more impaired RV systolic function (evaluated with both TAPSE and RV free wall strain).

Univariable Cox regression analysis was performed to characterize the relation between patient characteristics and outcomes. As shown in Table 3, NYHA class III to IV heart failure symptoms, amyloidosis phenotype, LVEF, stroke

Table 2
Echocardiographic characteristics

| Variable | Total (n=93) | Survivors (n=51) | Nonsurvivors (n=42) | p value |
|---|---------------|------------------|---------------------|---------|
| Interventricular septum thickness (mm) | 15 (13–17) | 15 (13–17) | 15 (14–17) | 0.602 |
| LV end-diastolic diameter (mm) | 44 (40–48) | 45 (41–49) | 43 (38–48) | 0.169 |
| LV end-diastolic volume (ml/m ²) | 52 ± 17 | 53 ± 16 | 50 ± 18 | 0.398 |
| LV mass (g/m ²) | 131 (101–170) | 130 (101–165) | 139 (100–177) | 0.663 |
| Left atrial volume (ml/m ²) | 37 (19–52) | 45 (26–53) | 23 (15–49) | 0.005 |
| LV ejection fraction (%) | 60 (50–65) | 61 (50–65) | 59 (47–64) | 0.419 |
| Stroke volume (ml/m ²) | 34.8 ± 11.8 | 39.3 ± 12.0 | 30.2 ± 9.6 | 0.001 |
| LV global longitudinal strain (%) | 13 ± 4 | 13 ± 3 | 12 ± 5 | 0.090 |
| LV apical ratio ≥ 1 | 36 (40%) | 12 (26%) | 24 (57%) | 0.002 |
| RV free wall thickness (mm) | 7 (6–9) | 7 (6–9) | 7 (6–9) | 0.254 |
| E/A | 1.1 (0.7–1.5) | 1.2 (0.8–1.7) | 0.9 (0.6–1.3) | 0.024 |
| E/e' | 15 (10–21) | 12 (8–16) | 18 (13–27) | <0.001 |
| E/e' > 14 | 40 (51%) | 16 (36%) | 24 (69%) | 0.004 |
| E deceleration time (ms) | 181 (152–236) | 188 (154–249) | 178 (151–227) | 0.442 |
| PA systolic pressure (mm Hg) | 36 ± 12 | 36 ± 11 | 35 ± 13 | 0.809 |
| Right atrial volume (ml/m ²) | 23 (13–38) | 28 (17–41) | 16 (12–30) | 0.009 |
| RV basal diameter (mm) | 38 ± 7 | 38 ± 6 | 38 ± 7 | 0.934 |
| RV mid diameter (mm) | 29 ± 6 | 29 ± 5 | 29 ± 6 | 0.860 |
| Tricuspid annular plane systolic excursion (mm) | 18 ± 6 | 20 ± 5 | 15 ± 5 | <0.001 |
| Tricuspid annular plane systolic excursion <17 mm | 41 (45%) | 15 (29%) | 26 (63%) | 0.001 |
| Fractional area change (%) | 41 ± 9 | 42 ± 8 | 40 ± 10 | 0.338 |
| Fractional area change < 35% | 20 (23%) | 8 (17%) | 12 (29%) | 0.156 |
| RV free wall strain (%) | 18 (14–24) | 22 (17–26) | 14 (11–18) | <0.001 |
| RV free wall strain < 16% | 33 (35%) | 7 (14%) | 26 (62%) | <0.001 |

LV = left ventricular; PA = pulmonary artery; RV = right ventricular.

Table 3
Univariable Cox regression analysis for all-cause mortality

| Variable | Univariable analysis | | |
|---|----------------------|-----------|---------|
| | HR | 95% CI | p value |
| Age | 1.01 | 0.98–1.03 | 0.606 |
| Male | 0.68 | 0.34–1.34 | 0.261 |
| New York Heart Association class III-IV | 2.42 | 1.30–4.51 | 0.005 |
| Amyloid light-chain type | 1.87 | 1.02–3.45 | 0.044 |
| Body mass index | 0.94 | 0.85–1.03 | 0.193 |
| Diabetes mellitus | 1.02 | 0.43–2.44 | 0.960 |
| Hypertension | 0.61 | 0.32–1.17 | 0.135 |
| Dyslipidemia | 0.81 | 0.40–1.64 | 0.562 |
| Atrial fibrillation | 1.37 | 0.68–2.75 | 0.379 |
| Beta blockers | 0.67 | 0.36–1.24 | 0.198 |
| Renin angiotensin aldosterone system inhibitors | 0.53 | 0.27–1.04 | 0.066 |
| Diuretic | 1.65 | 0.83–3.29 | 0.157 |
| Mineralocorticoid receptor antagonists | 1.01 | 0.53–1.95 | 0.973 |
| Statin | 0.56 | 0.29–1.10 | 0.095 |
| Anti-arrhythmic | 1.11 | 0.44–2.84 | 0.824 |
| Interventricular septum thickness | 1.06 | 0.97–1.16 | 0.201 |
| Left ventricular end-diastolic diameter | 0.97 | 0.92–1.01 | 0.167 |
| Left ventricular mass | 1.00 | 1.00–1.01 | 0.242 |
| Left atrial volume | 0.99 | 0.97–1.01 | 0.253 |
| Right atrial volume | 0.99 | 0.97–1.01 | 0.289 |
| Left ventricular ejection fraction | 0.98 | 0.95–1.00 | 0.047 |
| Stroke volume | 0.95 | 0.92–0.99 | 0.005 |
| Left ventricular global longitudinal strain | 0.89 | 0.82–0.97 | 0.010 |
| Left ventricular apical ratio ≥ 1 | 0.91 | 1.04–3.53 | 0.039 |
| Tricuspid annular plane systolic excursion | 0.91 | 0.87–0.97 | 0.001 |
| Fractional area change | 0.96 | 0.92–0.99 | 0.020 |
| Right ventricular free wall strain | 0.88 | 0.84–0.93 | <0.001 |
| Mean E/e' | 1.04 | 1.02–1.06 | <0.001 |
| Pulmonary artery systolic pressure | 1.02 | 0.98–1.05 | 0.319 |

volume index, LV GLS, LV apical ratio, TAPSE, RV fractional area change, RV free wall strain, and mean E/e' ratio were all associated with all-cause mortality. Due to the limited number of events to avoid overfitting, several multivariable Cox regression models were built and RV free wall strain remained independently associated with all-cause mortality in all of them (Table 4). As shown in Figure 1, both conventional and advanced parameters of RV systolic function showed incremental prognostic value when added to a basal model (including NYHA functional class, amyloidosis phenotype, and LV GLS). The model that included advanced parameters of RV systolic function (i.e., RV free wall strain) showed the highest predictivity (i.e., chi-square value) compared with the other parameters of RV systolic function.

To further investigate the relation between all-cause mortality and RV free wall strain, a spline curve was fitted. As shown in Figure 2, the HR for all-cause mortality steadily increased from lower to higher values of RV free wall strain and was equal to 1 (neutral effect) at 16%. The use of 16% as a prognostic cut-off value of RV free wall strain was also supported by the receiver operating characteristic curve and Youden index which was the highest at 16% (with a sensitivity of 0.863 and a specificity of 0.643 to predict patient survival). At baseline echocardiographic assessment, 60 patients (65%) presented with preserved RV systolic function (RV free wall strain $\geq 16\%$), whereas 33 (35%) had impaired RV systolic function (RV free wall strain $<16\%$). During follow-up, 23 of all deaths (55%) occurred in the first 12 months, including 16 deaths in patients with RV systolic impairment. The overall 1- and 3-year cumulative survival rates were 63% and 49%, respectively. The Kaplan-Meier curves showed significantly lower

Table 4
Multivariable Cox regression models for all-cause mortality

| Variable | Multivariable model 1 | | | Multivariable model 2 | | | Multivariable model 3 | | |
|-------------------|-----------------------|-----------|---------|-----------------------|-----------|---------|-----------------------|-----------|---------|
| | HR | 95% CI | P value | HR | 95% CI | P value | HR | 95% CI | P value |
| NYHA class III-IV | 1.38 | 0.72–2.64 | 0.336 | 1.85 | 0.94–3.63 | 0.076 | 1.35 | 0.63–2.91 | 0.443 |
| AL type | 2.23 | 1.15–4.29 | 0.017 | 1.98 | 1.05–3.75 | 0.035 | 1.81 | 0.93–3.53 | 0.082 |
| SVi | | | | | | | 0.98 | 0.94–1.02 | 0.222 |
| LV GLS | 0.92 | 0.86–0.99 | 0.021 | | | | | | |
| TAPSE | | | | 0.92 | 0.87–0.98 | 0.005 | | | |
| RV FWS | 0.89 | 0.84–0.95 | <0.001 | 0.90 | 0.85–0.96 | 0.001 | 0.89 | 0.83–0.95 | <0.001 |
| Variable | Multivariable model 4 | | | Multivariable model 5 | | | Multivariable model 6 | | |
| | HR | 95% CI | P value | HR | 95% CI | P value | HR | 95% CI | P value |
| NYHA class III-IV | 1.83 | 0.91–3.69 | 0.089 | 1.17 | 0.49–2.81 | 0.730 | 1.55 | 0.79–3.05 | 0.201 |
| LVEF | 1.00 | 0.97–1.03 | 0.826 | | | | | | |
| SVi | | | | 0.98 | 0.94–1.02 | 0.332 | | | |
| LV AR ≥ 1 | | | | | | | 1.15 | 0.58–2.28 | 0.682 |
| TAPSE | 0.93 | 0.88–0.99 | 0.024 | | | | | | |
| FAC | | | | | | | 0.98 | 0.94–1.02 | 0.324 |
| RV FWS | 0.91 | 0.86–0.97 | 0.002 | 0.89 | 0.83–0.96 | 0.003 | 0.91 | 0.86–0.97 | 0.005 |
| E/e' | | | | 1.03 | 1.00–1.05 | 0.021 | | | |

AL = amyloid light-chain; FAC = fractional area change; LV AR = left ventricular apical ratio; LVEF = left ventricular ejection fraction; LV GLS = left ventricular global longitudinal strain; NYHA = New York Heart Association; RV FWS = right ventricular free wall strain; SVi = stroke volume index; TAPSE = tricuspid annular plane systolic excursion.

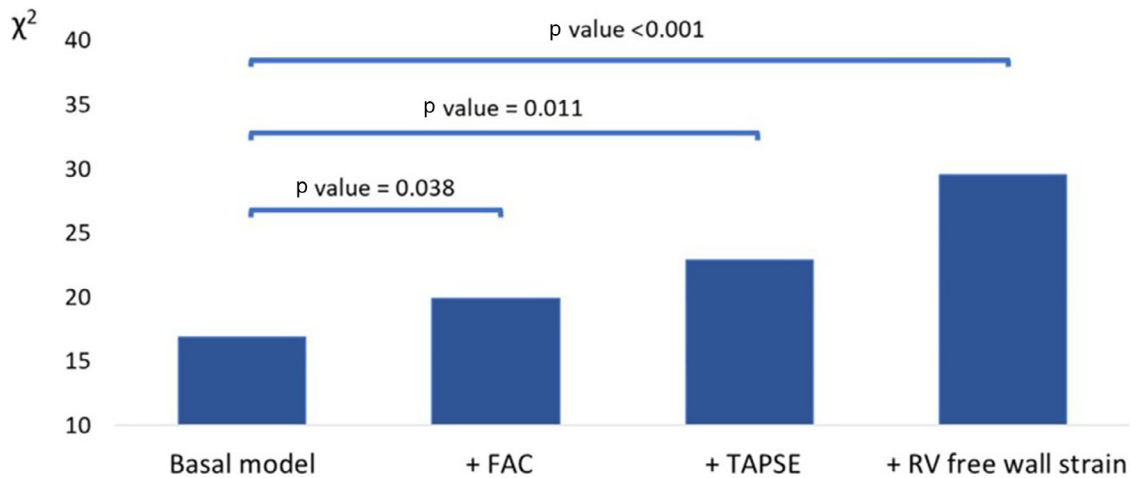


Figure 1. Incremental prognostic value of RV free wall strain over conventional parameters of RV systolic function. The bar charts represent the predictivity (chi-square) of several multivariable Cox regression models. The basal model includes heart failure symptoms, amyloidosis phenotype, and left ventricular global longitudinal strain. The addition of RV free wall strain to the basal model yielded a higher increment in predictivity compared with conventional parameters of RV systolic function. FAC = fractional area change.

short- and long-term survival rates in patients with RV systolic dysfunction than those with preserved RV systolic function (1- and 3-year cumulative survival: 81% vs 31% and 67% vs 20%, respectively; overall log-rank chi-square: 28.33, $p < 0.001$) (Figure 3).

Discussion

The main findings of the present study can be summarized as follows: (1) both standard (TAPSE) and advanced (RV free wall strain) echocardiographic parameters of RV

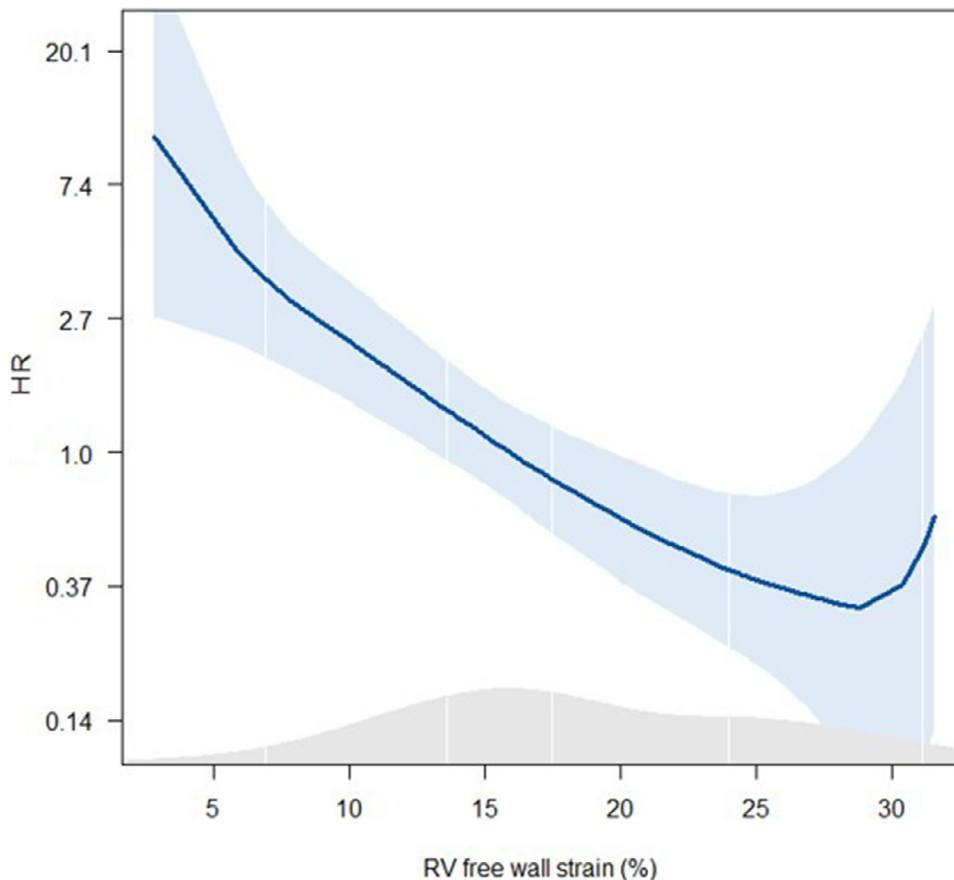


Figure 2. Spline curve analysis for all-cause mortality versus baseline RV free wall strain. The blue line represents the HR for all-cause mortality (with the overlaid 95% confidence intervals) according to the values of RV free wall strain. The gray density plot at the bottom of the figure illustrates the patient distribution according to RV free wall strain. The figure demonstrates that lower values of RV free wall strain were associated with higher risk of all-cause mortality.

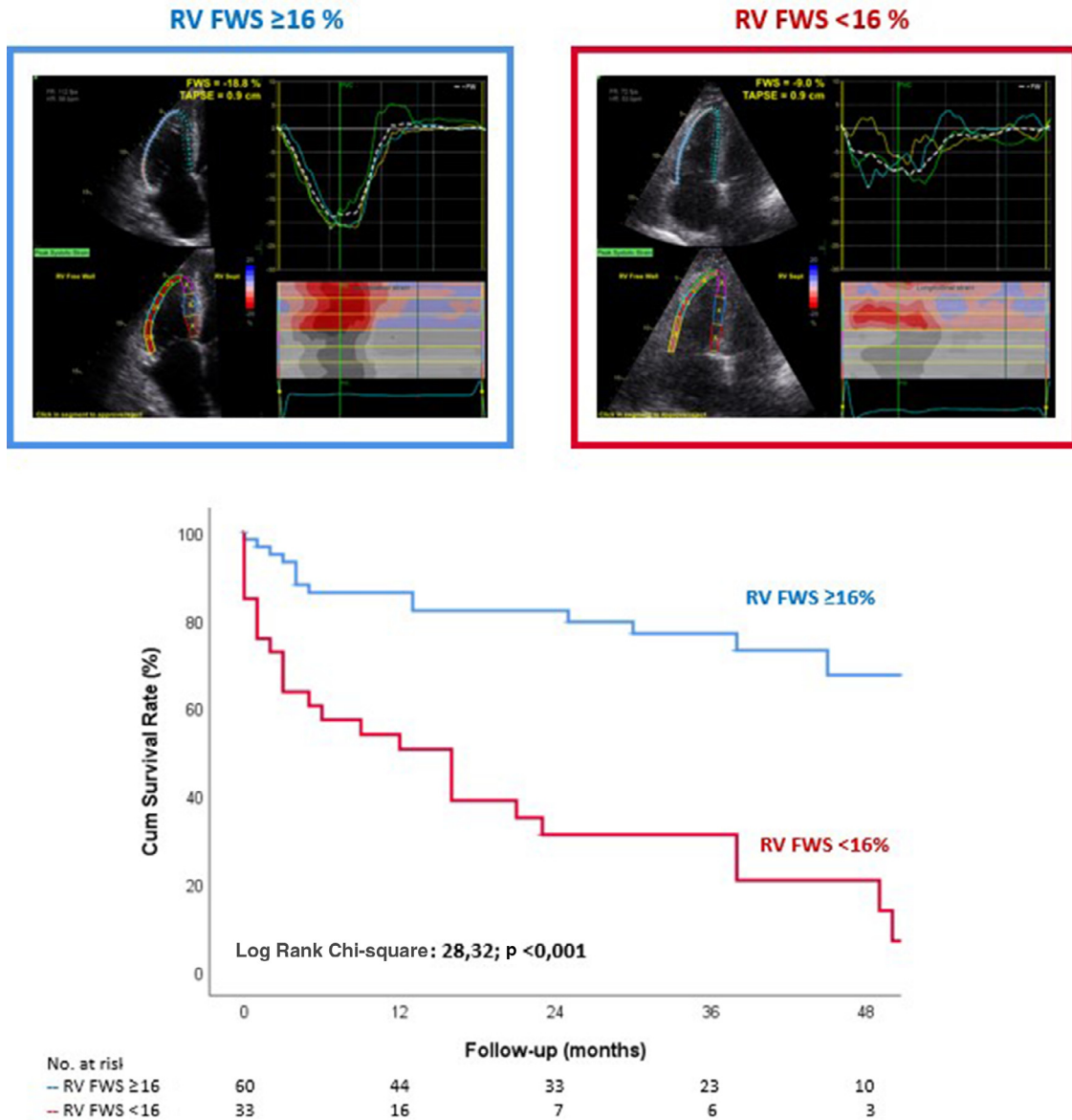


Figure 3. RV FWS and survival in cardiac amyloidosis. The Kaplan-Meier curves show that patients with impaired RV FWS (light-blue line and box) had significantly worse survival during the follow-up compared with patients with preserved RV FWS (red line and box). FWS = free wall strain.

systolic function show an independent association with all-cause mortality in patients with CA, even after adjusting for LV GLS, HF symptoms and amyloidosis phenotype; (2) RV free wall strain demonstrates the strongest association with all-cause mortality and has incremental prognostic value over conventional parameters of RV systolic function; and (3) an RV free wall strain cut-off value of 16% shows the greatest sensitivity and specificity to predict patient survival and may improve risk stratification of patients with CA.

Amyloidosis is a disease caused by misfolded proteins that aggregate and deposit as amyloid fibrils. The type of amyloidosis is based on the biochemical nature of the protein with the 2 most common types being AL and ATTR amyloidosis.³ It is well known that cardiac involvement is common in these patients and it is the cardiac involvement that drives prognosis regardless of the subtype of

amyloidosis.¹² Most studies, however, have only focused on LV involvement.^{13,14} Nonetheless, the prognostic value of RV systolic dysfunction in patients with heart failure (both with reduced and preserved LVEF) is increasingly recognized.^{15,16} RV systolic dysfunction may aggravate heart failure symptoms and increases the risk of cardiovascular events by reducing LV cardiac output (through a reduction in LV preload), thereby enhancing neurohormonal activation and compromising end-organ perfusion.^{17,18} RV systolic dysfunction may also lead to venous congestion, leading to renal impairment and hepatic dysfunction.¹⁹ In patients with CA, 2 potential mechanisms may explain RV involvement: (1) primary RV infiltration and (2) an increase in RV afterload resulting from LV systolic and diastolic dysfunction, which leads to retrograde transmission of elevated left-sided filling pressures, pulmonary hypertension, and pulmonary

vascular remodeling. Although RV abnormalities have been described in patients with CA,²⁰ less is known about the prognostic value of RV systolic function in these patients. In 322 patients with CA, Knight et al²¹ demonstrated that impaired TAPSE was independently associated with worse outcomes. Similarly, in 74 patients with biopsy-proved AL amyloidosis, Ghio et al²² showed that TAPSE <17 mm was the only echocardiographic parameter associated with poor survival.

Although the presence of impaired RV systolic function seems strongly associated with worse outcome, detection of RV systolic dysfunction by conventional echocardiography (i.e., TAPSE) remains difficult. TAPSE only measures the displacement of the lateral annulus, thereby extrapolating the motion of a single point to the entire ventricle. In addition, TAPSE is angle- and load-dependent and regional differences (which are well known in patients with CA) cannot be identified. In contrast, RV free wall strain is less angle- and volume-dependent and is known to have a high sensitivity for detecting (subclinical) RV systolic dysfunction.²³ In 880 patients with heart failure, Morris et al²⁴ demonstrated that RV strain was more sensitive than TAPSE in detecting RV systolic dysfunction. RV free wall strain also showed a better correlation with RV EF measured with cardiac magnetic resonance imaging.²⁵ In 93 patients with CA, Fine et al⁵ showed that RV free wall strain was significantly associated with the primary end point of all-cause mortality or cardiovascular hospitalization. However, the incremental value of RV free wall strain over traditional parameters of RV systolic function (i.e., TAPSE) was not shown. The present study is in line with these observations and shows the incremental value of RV free wall strain over TAPSE.

Novel treatment options are emerging that could improve prognosis in patients with CA. However, these treatments are expensive and seem most efficient when started at an early stage of the disease.²⁶ A widely spread imaging technique such as echocardiography can help to timely identify patients with CA and improve risk stratification in these patients. The present study shows that evaluation of RV involvement by advanced imaging techniques (i.e., RV free wall strain) improves risk stratification and should be part of the integrated assessment of CA. Prospective studies are needed to evaluate the response of the RV during treatment, which may be helpful to identify patients in whom continuation of treatment seems useful or futile.

This study is limited by the retrospective, observational design. A time span of 20 years was used for inclusion of patients to acquire the large cohort as presented. Cardiac magnetic resonance imaging was not performed for comparison with RV free wall strain measurements. Assessment of RV free wall strain is vendor-dependent, and values cannot be compared across different ultrasound platforms. Heart failure hospitalization as an end point was not available, and it was not possible to differentiate between cardiac and noncardiac causes of mortality.

In conclusion, RV systolic dysfunction is independently associated with poor outcomes in patients with CA and the use of advanced echocardiographic parameters, such as RV free wall strain, provides incremental prognostic value compared with conventional echocardiographic parameters such as TAPSE.

Disclosures

Dr. Bax received speaking fees from Abbott Vascular. Dr. Marsan received speaking fees from Abbott Vascular and GE Healthcare. Dr. Delgado received speaker fees from Abbott Vascular, Medtronic, Merck Sharp & Dohme, Edwards Lifesciences, and GE Healthcare (Little Chalfont, United Kingdom). The remaining authors have no conflicts of interest to declare.

- Pande M, Srivastava R. Molecular and clinical insights into protein misfolding and associated amyloidosis. *Eur J Med Chem* 2019; 184:111753.
- Quarta CC, Kruger JL, Falk RH. Cardiac amyloidosis. *Circulation* 2012;126:e178–e182.
- Fontana M, Corović A, Scully P, Moon JC. Myocardial amyloidosis: the exemplar interstitial disease. *JACC Cardiovasc Imaging* 2019;12:2345–2356.
- Witteles RM, Liedtke M. AL amyloidosis for the cardiologist and oncologist: epidemiology, diagnosis, and management. *JACC Cardio-oncol* 2019;1:117–130.
- Fine NM, White JA, Jimenez-Zepeda V, Howlett JG. Determinants and prognostic significance of serial right heart function changes in patients with cardiac amyloidosis. *Can J Cardiol* 2020;36:432–440.
- Uzan C, Lairez O, Raud-Raynier P, Garcia R, Degand B, Christiaens LP, Rehman MB. Right ventricular longitudinal strain: a tool for diagnosis and prognosis in light-chain amyloidosis. *Amyloid* 2018;25:18–25.
- Dorbala S, Ando Y, Bokhari S, Dispenzieri A, Falk RH, Ferrari VA, Fontana M, Gheysens O, Gillmore JD, Glaudemans AWJM, Hanna MA, Hazenberg BPC, Kristen AV, Kwong RY, Maurer MS, Merlini G, Miller EJ, Moon JC, Murthy VL, Quarta CC, Rapezzi C, Ruberg FL, Shah SJ, Slart RHJA, Verberne HJ, Bourque JM. ASNC/AHA/ASE/EANM/HFSA/ISA/SCMR/SNMMI Expert Consensus recommendations for multimodality imaging in cardiac amyloidosis: part 1 of 2-evidence base and standardized methods of imaging. *J Nucl Cardiol* 2019;26:2065–2123.
- Lang RM, Badano LP, Mor-Avi V, Filalo J, Armstrong A, Ernande L, Flachskampf FA, Foster E, Goldstein SA, Kuznetsova T, Lancellotti P, Muraru D, Picard MH, Rietzschel ER, Rudski L, Spencer KT, Tsang W, Voigt JU. Recommendations for cardiac chamber quantification by echocardiography in adults: an update from the American Society of Echocardiography and the European Association of Cardiovascular Imaging. *J Am Soc Echocardiogr* 2015;28: 1–39.e14.
- Zoghbi WA, Adams D, Bonow RO, Enriquez-Sarano M, Foster E, Grayburn PA, Hahn RT, Han Y, Hung J, Lang RM, Little SH, Shah DJ, Sherman S, Thavendiranathan P, Thomas JD, Weissman NJ. Recommendations for noninvasive evaluation of native valvular regurgitation: a report from the American Society of Echocardiography developed in collaboration with the Society for Cardiovascular Magnetic Resonance. *J Am Soc Echocardiogr* 2017;30:303–371.
- Badano LP, Koliás TJ, Muraru D, Abraham TP, Aurigemma G, Edvardsen T, D'Hooge J, Donal E, Fraser AG, Marwick T, Mertens L, Popescu BA, SenGupta PP, Lancellotti P, Thomas JD, Voigt JU. Industry representatives, Reviewers: This document was reviewed by members of the 2016–2018 EACVI Scientific Documents Committee. Standardization of left atrial, right ventricular, and right atrial deformation imaging using two-dimensional speckle tracking echocardiography: a consensus document of the EACVI/ASE/Industry Task Force to standardize deformation imaging. *Eur Heart J Cardiovasc Imaging* 2018;19:591–600.
- Cyrille NB, Goldsmith J, Alvarez J, Maurer MS. Prevalence and prognostic significance of low QRS voltage among the three main types of cardiac amyloidosis. *Am J Cardiol* 2014;114:1089–1093.
- Falk RH, Comenzo RL, Skinner M. The systemic amyloidoses. *N Engl J Med* 1997;337:898–909.
- Senapati A, Sperry BW, Grodin JL, Kusunose K, Thavendiranathan P, Jaber W, Collier P, Hanna M, Popovic ZB, Phelan D. Prognostic implication of relative regional strain ratio in cardiac amyloidosis. *Heart* 2016;102:748–754.

14. Koyama J, Falk RH. Prognostic significance of strain Doppler imaging in light-chain amyloidosis. *JACC Cardiovasc Imaging* 2010;3:333–342.
15. Ghio S, Gavazzi A, Campana C, Inserra C, Klersy C, Sebastiani R, Arbustini E, Recusani F, Tavazzi L. Independent and additive prognostic value of right ventricular systolic function and pulmonary artery pressure in patients with chronic heart failure. *J Am Coll Cardiol* 2001;37:183–188.
16. Mohammed SF, Hussain I, Abouezzeddine OF, Takahama H, Kwon SH, Forfia P, Roger VL, Redfield MM. Right ventricular function in heart failure with preserved ejection fraction: a community-based study. *Circulation* 2014;130:2310–2320.
17. Voelkel NF, Quaife RA, Leinwand LA, Barst RJ, McGoon MD, Meldrum DR, Dupuis J, Long CS, Rubin LJ, Smart FW, Suzuki YJ, Gladwin M, Denholm EM, Gail DB, National Heart, Lung, and Blood Institute Working Group on Cellular and Molecular Mechanisms of Right Heart Failure. Right ventricular function and failure: report of a National Heart, Lung, and Blood Institute Working Group on Cellular and Molecular Mechanisms of Right Heart Failure. *Circulation* 2006;114:1883–1891.
18. Meyer P, Filippatos GS, Ahmed MI, Iskandrian AE, Bittner V, Perry GJ, White M, Aban IB, Mujib M, Dell'Italia LJ, Ahmed A. Effects of right ventricular ejection fraction on outcomes in chronic systolic heart failure. *Circulation* 2010;121:252–258.
19. Tang WH, Mullens W. Cardiorenal syndrome in decompensated heart failure. *Heart* 2010;96:255–260.
20. Arvidsson S, Henein MY, Wikström G, Suhr OB, Lindqvist P. Right ventricular involvement in transthyretin amyloidosis. *Amyloid* 2018;25:160–166.
21. Knight DS, Zumbo G, Barcella W, Steeden JA, Muthurangu V, Martinez-Naharro A, Treibel TA, Abdel-Gadir A, Bulluck H, Kotecha T, Francis R, Rezk T, Quarta CC, Whelan CJ, Lachmann HJ, Wechalekar AD, Gillmore JD, Moon JC, Hawkins PN, Fontana M. Cardiac structural and functional consequences of amyloid deposition by cardiac magnetic resonance and echocardiography and their prognostic roles. *JACC Cardiovasc Imaging* 2019;12:823–833.
22. Ghio S, Perlini S, Palladini G, Marsan NA, Faggiano G, Vezzoli M, Klersy C, Campana C, Merlini G, Tavazzi L. Importance of the echocardiographic evaluation of right ventricular function in patients with AL amyloidosis. *Eur J Heart Fail* 2007;9:808–813.
23. Rudski LG, Lai WW, Afilalo J, Hua L, Handschumacher MD, Chandrasekaran K, Solomon SD, Louie EK, Schiller NB. Guidelines for the echocardiographic assessment of the right heart in adults: a report from the American Society of Echocardiography, a registered branch of the European Society of Cardiology, and the Canadian Society of Echocardiography. *J Am Soc Echocardiogr* 2010;23:685–788.
24. Morris DA, Krisper M, Nakatani S, Köhncke C, Otsuji Y, Belyavskiy E, Radha Krishnan AK, Kropf M, Osmanoglou E, Boldt LH, Blaschke F, Edelmann F, Haverkamp W, Tschöpe C, Pieske-Kraigher E, Pieske B, Takeuchi M. Normal range and usefulness of right ventricular systolic strain to detect subtle right ventricular systolic abnormalities in patients with heart failure: a multicentre study. *Eur Heart J Cardiovasc Imaging* 2017;18:212–223.
25. Park JH, Negishi K, Kwon DH, Popovic ZB, Grimm RA, Marwick TH. Validation of global longitudinal strain and strain rate as reliable markers of right ventricular dysfunction: comparison with cardiac magnetic resonance and outcome. *J Cardiovasc Ultrasound* 2014; 22:113–120.
26. Maurer MS, Schwartz JH, Gundapaneni B, Elliott PM, Merlini G, Waddington-Cruz M, Kristen AV, Grogan M, Wittes R, Damy T, Drachman BM, Shah SJ, Hanna M, Judge DP, Barsdorf AI, Huber P, Patterson TA, Riley S, Schumacher J, Stewart M, Sultan MB, Rapezzi C, ATTR-ACT, Study Investigators. Tafamidis treatment for patients with transthyretin amyloid cardiomyopathy. *N Engl J Med* 2018; 379:1007–1016.